



Dynamic response analysis of story-adding structure with isolation technique subjected to near-fault pulse-like ground motions

X.T. Ma ^a  , C. Bao ^b, S.I. Doh ^c, H. Lu ^a, L.X. Zhang ^a, Z.W. Ma ^a, Y.T. He ^a

Show more 

 Outline |  Share  Cite

<https://doi.org/10.1016/j.pce.2020.102957>

[Get rights and content](#)

Highlights

- The dynamic response of structures under near-fault pulse-like ground motions and far-fault ground motions are studied.
- Isolation technique is applied in story-adding structures.
- The seismic performances of different story-adding schemes are studied and compared.
- Seismic response of the adding-story structure is amplified due to the higher altitude installation position of bearings.

Abstract

The isolation technique is widely studied and applied in structural engineering due to its excellent seismic performance. However, the existing research mostly focuses on the

conventional structure under the action of regular ground motions. In this paper, a story-adding seismic structure, a base-isolated structure, and a story-adding isolated structure were simulated by using numerical simulation methods. The dynamic response characteristics of the three structures under near-fault pulse-like ground motions are analysed and compared with the far-fault ground motions. The results showed that using the base isolation can significantly extend the period of the main structure and reduce the seismic response on the upper structure. The inter-story drift ratio, inter-story shear force, and the story acceleration of all three structures under near-field pulse-like ground motions were all larger than that of far-field earthquakes. Both base-isolated structure and story-adding isolated structure showed excellent damping performance. Besides, the damping properties of the base-isolated structure are better than the story-adding isolated structure.

 Previous

Next 

Keywords

Dynamic response analysis; Isolation technique; Near-fault earthquake; Pulse-like ground motion; Story isolation; Time-history analysis

1. Introduction

As one of the most effective and successful seismic protection techniques ([Makris, 2019](#)), the seismic isolation technique has dramatically developed and widely applied in various buildings and bridges. However, due to the uncertainty of earthquakes and the increasing complexity of structures, seismic isolation technique faces many problems and challenges that need to be solved. In the last few years, a lot of research work has been carried out mainly on some unusual structures, such as liquid storage tanks ([Saha et al., 2016](#); [Waghmare et al., 2019](#); [Zhang et al., 2011](#); [Cheng et al., 2017](#); [Luo et al., 2016](#)), tunnels ([Hasheminejad and Miri, 2008](#); [Chen and Shen, 2014](#); [Ma et al., 2018](#); [Xu et al., 2020](#)), spatial structures ([Yong-Chul et al., 2010](#); [Li et al., 2013](#); [Cai et al., 2016](#); [Zhang et al., 2019](#)), and even retrofit of some historic buildings ([Branco and Guerreiro, 2011](#); [Petrovčič and Kilar, 2017](#); [Lupășteanu et al., 2019](#); [Lignola et al., 2016](#)). However, the retrofit of existing building structures is mostly limited to the application of the base isolation technique ([Kanyilmaz and Castiglioni, 2017](#); [Mansouri and Nazari, 2017](#); [Ferraioli and Mandara, 2016](#)).

For some special buildings, the inter-story isolation technique, which also called the mid-story isolation technique, is much more effective to meet the seismic demands. Chey, M. H., et al. ([Chey et al., 2013](#)) utilized the isolation technique in storey-adding reconstruction of the existing structure to control the seismic response of entire structure. Wang, S. J. et al. ([Wang et al., 2012](#)) studied the Differences in seismic response between isolated structures and mid-isolated structures by experiment method. Loh, C. H. et al. ([Loh et al., 2013](#)) us

environmental vibration test data and seismic response data to study the time-varying dynamic characteristics of story-isolated structures. To obtain the response characteristics of a simple two-degree-of-freedom model, Zhou, Q. et al. (Zhou et al., 2016) suggested a new method.

In the process of the rapid development of urban construction, the story-adding reconstruction project is gradually increasing. However, some studies show that the stiffness distribution of the original structure will be changed, and the whole structure will be more complicated after adding several stories. The result shows that the natural period and the inter-story drift ratio of the story-adding structure increases; obviously, the torsional effect is more significant, some of which exceeded the specification limits (Lu and Chen, 2018; Li, 2014).

The isolation technique is applied in the story-adding reconstruction project, which can better exert the advantages of the isolated structural system, and has a good damping effect on the story-adding structure system. Like other isolated structures, lots of questions about inter-story-isolated structures also need to solve (Yan and Chen, 2015).

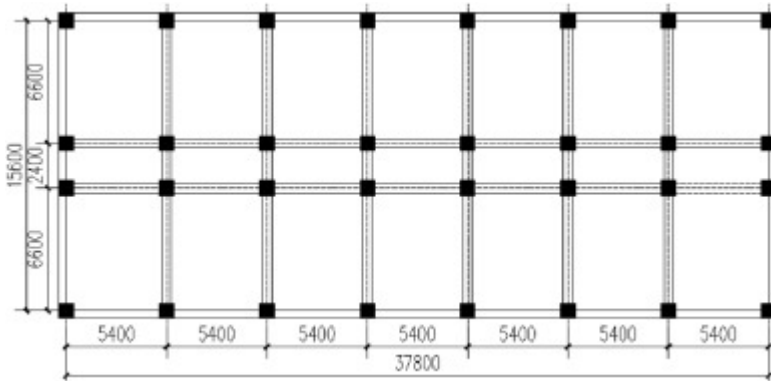
In recent decades, there have been some near-field earthquakes with great destructive powers in the world, such as the 1989 Loma Prieta earthquake and the 1994 Northridge earthquake in the United States, the 1995 Kobe earthquake in Japan, the 1999 Kocaeli earthquake in Turkey, and the 1999 Chi-Chi earthquake in Taiwan. All these earthquakes which have characteristics of strong directionality, long-period velocity, displacement pulse-like, and large peak acceleration caused serious damage to the structure (Wald et al., 1996; Rao and Jangid, 2001; Alonso-Rodríguez and Miranda, 2015; Almufti et al., 2015). The structure is subjected to high seismic energy impact, resulting in greater deformation and displacement (Chioccarelli and Iervolino, 2013). Compared with far-field ground motions, such ground motions with short time and high-energy are more likely to cause structural damage. Therefore, the higher seismic requirements of buildings are proposed. The strong destructiveness of the near-field pulse-like ground motions has attracted the attention of scholars, but the current research is not profound enough, and the theoretical research on the seismic performance of the structure under near-field earthquakes is not perfect. Due to a large number of seismic belts in China, many cities are in the vicinity of faults or fault zones. This requires us to consider the impact of near-field earthquakes on the structural response when conducting structural seismic response analysis. It is essential to study the seismic performance of different forms structures under near-fault earthquake condition.

In this paper, the near-field earthquakes with pulse-like components were selected, and the dynamic response condition and seismic response law of adding story structure using the base isolation and story isolation technique by elastoplastic time-history analysis method were studied, and study result the far-field ground motion. In this way, the researchers can further understand the near-field ground motion characteristics of such structures and provide a theoretical reference for the application of isolation technique.

2. Material and methods

2.1. Structural analysis model and parameters

The analysis model in this paper is a 7- stories adding-structure, the first to fifth stories are Reinforced concrete frames, and the sixth to seventh stories are steel frames. The building has a length of 37.8 m and a width of 15.6 m. The bottom story height is 4.1 m, and the standard story height is 3.6 m, the plan view of structures is shown in Fig. 1. The longitudinal reinforcement of beam and column is HRB335, the stirrup is HPB300, the section size of the column is 550 mm × 550 mm, the beam section size is 500 mm × 250 mm, and 450 mm × 250 mm, and the thickness of concrete slab is 120 mm. The concrete strength of the beam, the plate, and the column are all C35, the wall is made of MU7.5 aerated concrete block, the thickness of the exterior wall is 300 mm, and the interior wall is 200 mm. The steel is Q345B, the steel column is H300 × 300 × 12, and the steel beam is H400 × 200 × 8 × 10. The seismic fortification intensity of the project area is 8°, the design basic seismic acceleration is 0.2 g, the design earthquake group is the third, and the basic wind pressure is 0.55 kN/m².



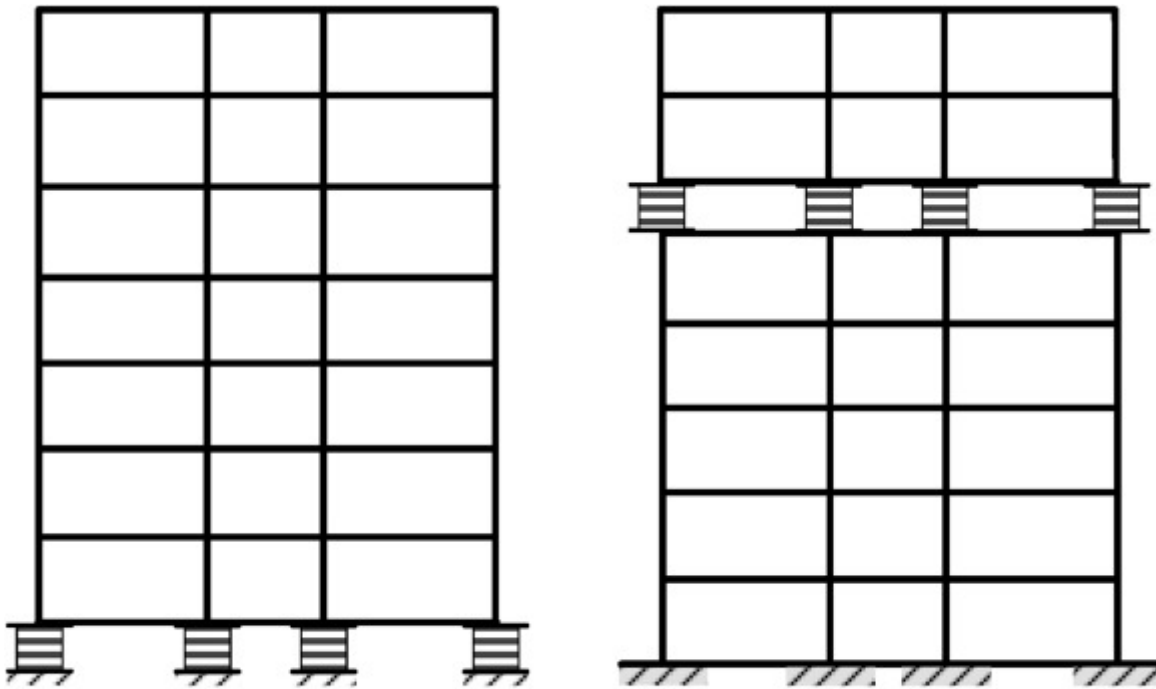
[Download : Download high-res image \(216KB\)](#)

[Download : Download full-size image](#)

Fig. 1. Plan view of structures.

2.2. Isolation method

The isolation method means that the isolation device installed on the base or a certain story of the building to dissipate earthquake energy. In this way, the seismic energy transmitted to the upper structure could be reduced, and the structural seismic response can also be mitigated, and only slight movement and deformation of the building will be caused. Thereby, it can ensure the structural safety during an earthquake, and the isolated model is shown in Fig. 2.



(a) Base-isolated structure.

(b) Story-isolated structure.

[Download : Download high-res image \(228KB\)](#)

[Download : Download full-size image](#)

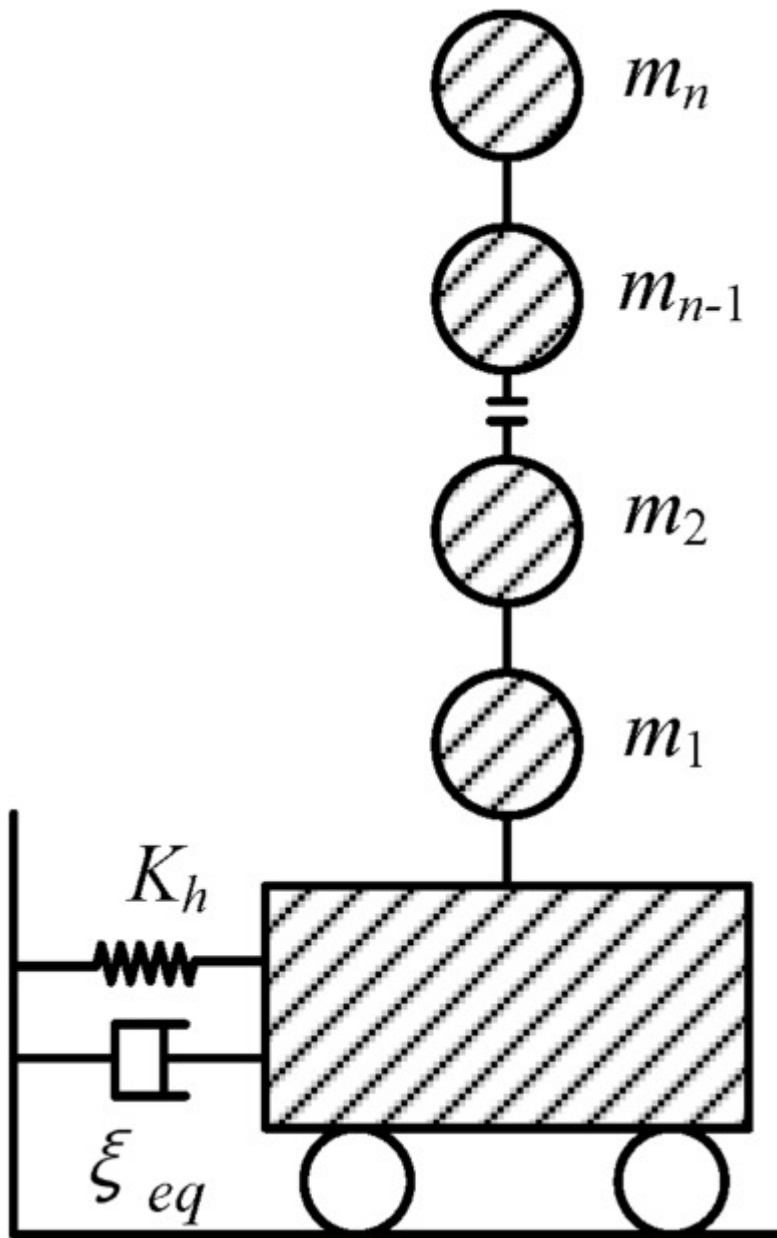
Fig. 2. Isolation model.

There are mainly three dynamic analysis models: a single-mass model, multi-mass model, or even spatial analysis model according to specific conditions, can be used as the isolated structure system. Because the horizontal stiffness of the upper structure is much larger than the isolators', the upper structure can be approximated as a rigid body, as a result, the isolated structure is simplified into a single-mass model for analysis. The dynamic equilibrium equation form is shown as Equation (1):

$$m\ddot{x} + c\dot{x} + kx = -m\ddot{x}_g \quad (1)$$

In Equation (1), m is the quality of structure; C is the damping coefficient and k is the horizontal stiffness of the isolation layer; \ddot{x} , \dot{x} and x are the acceleration, velocity, and displacement of the upper structure, respectively; \ddot{x}_g is the ground acceleration.

The multi-mass model and spatial analysis model consider the isolation layer as a structural mass, so they are always be used to analyse and acquire the detailed seismic response of the upper structure. For example, for the multi-mass model, the isolation layer can be simplified with a structural story of horizontal stiffness K_h and damping coefficient of c , as shown in Fig. 3.



[Download : Download high-res image \(365KB\)](#)

[Download : Download full-size image](#)

Fig. 3. Simplified diagram of isolated structure.

Among them, the horizontal dynamic stiffness calculation formula is below:

$$K_h = \sum_{i=1}^N K_i \quad (2)$$

In Equation (2), N is the number of isolation bearings, K_i is the horizontal dynamic stiffness of the i -th isolation bearing.

$$\xi_{eq} = \frac{\sum_{i=1}^N K_i \xi_i}{K_h} \quad (3)$$

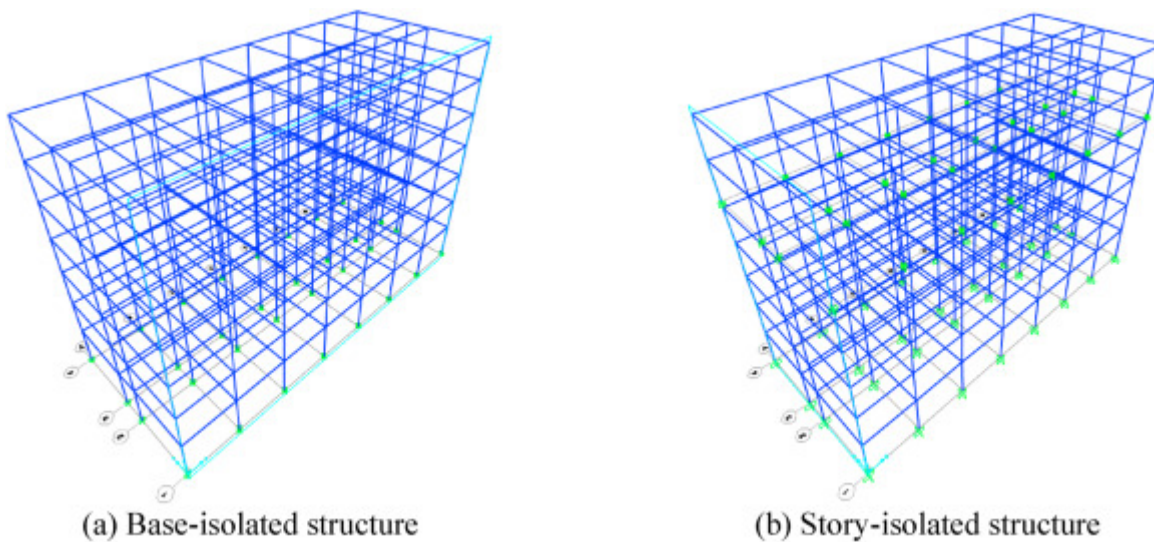
In Equation (3), ξ_i is the equivalent viscous damping ratio of the i -th isolation bearing.

In this way, the seismic response analysis of the isolated structure system can be performed by using both time-history analysis method and response spectrum method. However, the response spectrum curve should adjust by the damping ratio. The isolated structure can efficiently mitigate the horizontal seismic action of the structure above the isolation layer. The seismic codes and standard suggest the concept of horizontal damping coefficient to reflect mitigation condition of horizontal seismic action, and the horizontal seismic response of the isolated structure adopt a linear distribution in the direction of altitude. The maximum value of the horizontal seismic influence coefficient is the product of the maximum seismic influence coefficient of the non-isolated structure and the horizontal damping coefficient.

$$\alpha_{\max 1} = \beta \alpha_{\max} / \phi \quad (4)$$

In Equation (4), $\alpha_{\max 1}$ is the maximum of horizontal seismic influence coefficient after isolation; α_{\max} is the maximum of horizontal seismic influence coefficient of non-isolated structure; β is the horizontal damping coefficient; ϕ is the adjustment factor, generally 0.8 for the rubber support and 0.75 for the isolation bearing with the damper.

In this paper, the seismic structure, the base-isolated structure, and the adding-story structure with story isolation technique are established using SAP2000, respectively. The FE models of base-isolated structure and story-isolated structure are as shown in Fig. 4. The lead-laminated rubber bearings are used in all the isolated structures. The effective stiffness of the isolation layer is 882 kN/m, the effective damping is 0.272, the yielding force is 23.6 kN, and the post-yield stiffness ratio is 0.154.



[Download : Download high-res image \(1MB\)](#)

[Download : Download full-size image](#)

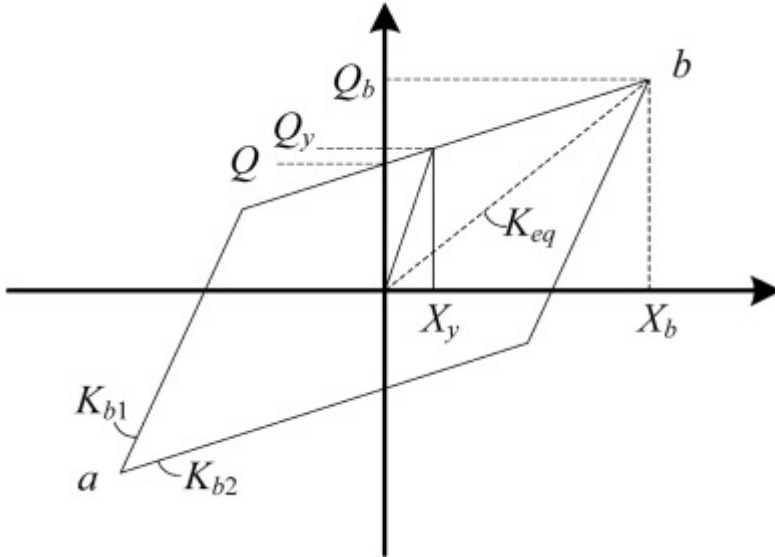
Fig. 4. FE models.

In the numerical model, the nonlinear hysteresis curve of the lead-laminated rubber isolation bearing (LRB) can be simplified as a bilinear model (Cai et al., 2016), as shown

5, the initial stiffness K_{b1} of the seismic isolation bearing and the post-yield stiffness K_{b2} are calculated as follows:

$$K_{b1} = \frac{Q_y}{X_y} \quad (5)$$

$$K_{b2} = \frac{(Q_b - Q_y)}{(X_b - X_y)} \quad (6)$$



[Download : Download high-res image \(181KB\)](#)

[Download : Download full-size image](#)

Fig. 5. Hysteresis model of the isolation bearing.

The point $b (X_b, Q_b)$ in Fig. 5 is the yield point of the lead-laminated rubber isolation bearing. The slope of the line connecting the two diagonal points a and b on the bilinear model is the equivalent horizontal shear stiffness K_{eq} , and its calculation equation is as follows:

$$K_{eq} = \frac{Q_b - Q_a}{X_b - X_a} \quad (7)$$

where, X_b is the maximum of positive horizontal displacement; X_a is the maximum of negative horizontal displacement; Q_b is the horizontal shear force corresponding to X_b ; Q_a is the horizontal shear force corresponding to X_a .

2.3. Selection of ground motion

Earthquake waves have complex spectral characteristics, compared with far-field earthquakes, near-fault pulse-like earthquakes have strong directional effects, sliding effects, upper plate effects, and characteristics of large-scale vertical acceleration. The two main causes of pulse-like recording are the forward directionality and the slipping effect in seismic fault rupture. Among them, the pulse-like effect is a concentrated expression of near-field ground motions. Thus, it is necessary to focus on the pulse-like effect. At present, there is no clear regional boundary for the division of near-field ground motions and far-field ground motions.

paper, the fault distance of less than 20 km is defined as the near-field region, which is the currently used value (Zhang et al., 2019). If different ground motions are put into a structural model, the seismic response will be very different. Sometimes the displacement and shear force of the structure will differ by several times or even several tens of times.

Therefore, a key factor of analysis results is the choice of the right seismic wave when conducting structural seismic analysis. In this paper, six near-field ground motions with pulse-like effects and six far-field earthquake waves were selected from the PEER by using the ATC-63 proposal. Moreover, the following principles were used when earthquake waves are selected: (1) The magnitude of the earthquake event is greater than 6.5. (2) For near-field pulse-like recording, the fault distance of the station where it is located does not exceed 10 km and has a distinct long-period pulse-like wave. (3) For far-field ground motions, the fault distance should be greater than 20 km (4) the peak ground accelerations are equal to or greater than 0.2 g. The selected near-field pulse-like earthquake records are not distinguished between directional effect and fault type. The specific parameters can be seen from Table 1. After selected the ground motions, the dynamic response of the seismic structure, the base-isolated structure, and the story-isolated structure under the near-field pulse-like ground motions were studied and compared with the far-field seismic response (see Table 2).

Table 1. Ground motion.

| | Earthquake waves | Earthquake events | Stations | Magnitude | Fault distance (km) | PGA (g) |
|-------------------------------------|------------------|-------------------|-----------------|-----------|---------------------|---------|
| Near-field pulse-like ground motion | NP-1 | Imperial Valley | Impvall/H-E06 | 6.5 | 0.6 | 0.44 |
| | NP-2 | Loma Prieta | Saratoga-Aloha | 6.9 | 7.6 | 0.38 |
| | NP-3 | Cape Mendocino | Petrolia | 7.0 | 8.5 | 0.63 |
| | NP-4 | Landers | Lucerne | 7.3 | 2.2 | 0.79 |
| | NP-5 | Chi-Chi | Tcu065 | 7.6 | 0.6 | 0.82 |
| | NP-6 | Duzce | Duzce | 7.1 | 0 | 0.52 |
| Far-field ground motion | F-1 | Imperial Valley | EI Centro Array | 6.5 | 25.2 | 0.38 |
| | F-2 | Kocaeli Turkey | Arelik | 7.5 | 23.8 | 0.22 |

| | Earthquake waves | Earthquake events | Stations | Magnitude | Fault distance (km) | PGA (g) |
|--|------------------|-------------------|--------------|-----------|---------------------|---------|
| | F-3 | Hector Mine | Hector | 7.1 | 22.5 | 0.34 |
| | F-4 | Kobe | Nishi-Akashi | 6.9 | 28.5 | 0.51 |
| | F-5 | Chi-Chi | CHY101 | 7.6 | 26.8 | 0.44 |
| | F-6 | Landers | Coolwater | 7.3 | 35.5 | 0.42 |

Table 2. Inter-story shear force (kN).

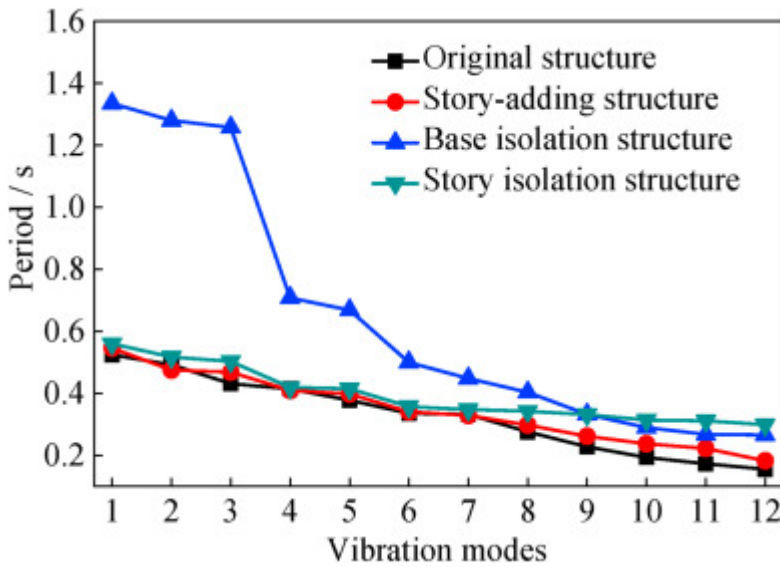
| | Near-field pulse-like ground motions | | | Far-field ground motions | | |
|---|--------------------------------------|-------------------------|--------------------------|--------------------------|-------------------------|--------------------------|
| | Seismic structure | base-isolated structure | story-isolated structure | Seismic structure | base-isolated structure | story-isolated structure |
| 1 | 11802.90 | 1550.56 | 5996.89 | 4582.05 | 1706.16 | 3538.81 |
| 2 | 10115.36 | 1684.27 | 5314.79 | 4065.82 | 1779.62 | 3014.53 |
| 3 | 8762.05 | 1461.08 | 4411.40 | 3264.81 | 1496.51 | 2352.76 |
| 4 | 7014.17 | 1018.52 | 3901.84 | 2822.32 | 1126.54 | 1906.42 |
| 5 | 4524.34 | 688.67 | 2608.97 | 2420.84 | 729.24 | 1332.05 |
| 6 | 1848.81 | 403.65 | 1204.79 | 1333.28 | 436.32 | 486.16 |
| 7 | 1097.72 | 228.75 | 466.79 | 841.20 | 261.85 | 297.64 |

3. Results and analysis

3.1. Analysis of the structural period

To understand the dynamic characteristics of structures with isolation technique under earthquake, the natural vibration characteristics of all these models are analysed before the time-history analysis, and the first twelve natural vibration period of the structure were obtained, which plotted in Fig. 6. With Fig. 6 revealed, the first several periods of the adding story structure are closer to the original structure, and the later periods are prolonged. The periods of the base-isolated structure are significantly prolonged, especially, the first three periods are prolonged even about 55%. Since the isolation bearings are installed at the top of the fifth story in the story-isolated structure, the periods are not prolonged significantly.

means that the natural vibration periods of the story-isolated structure are prolonged after installing the isolation bearings, and the seismic influence coefficient and the seismic response will both decline to a certain extent.



[Download : Download high-res image \(303KB\)](#)

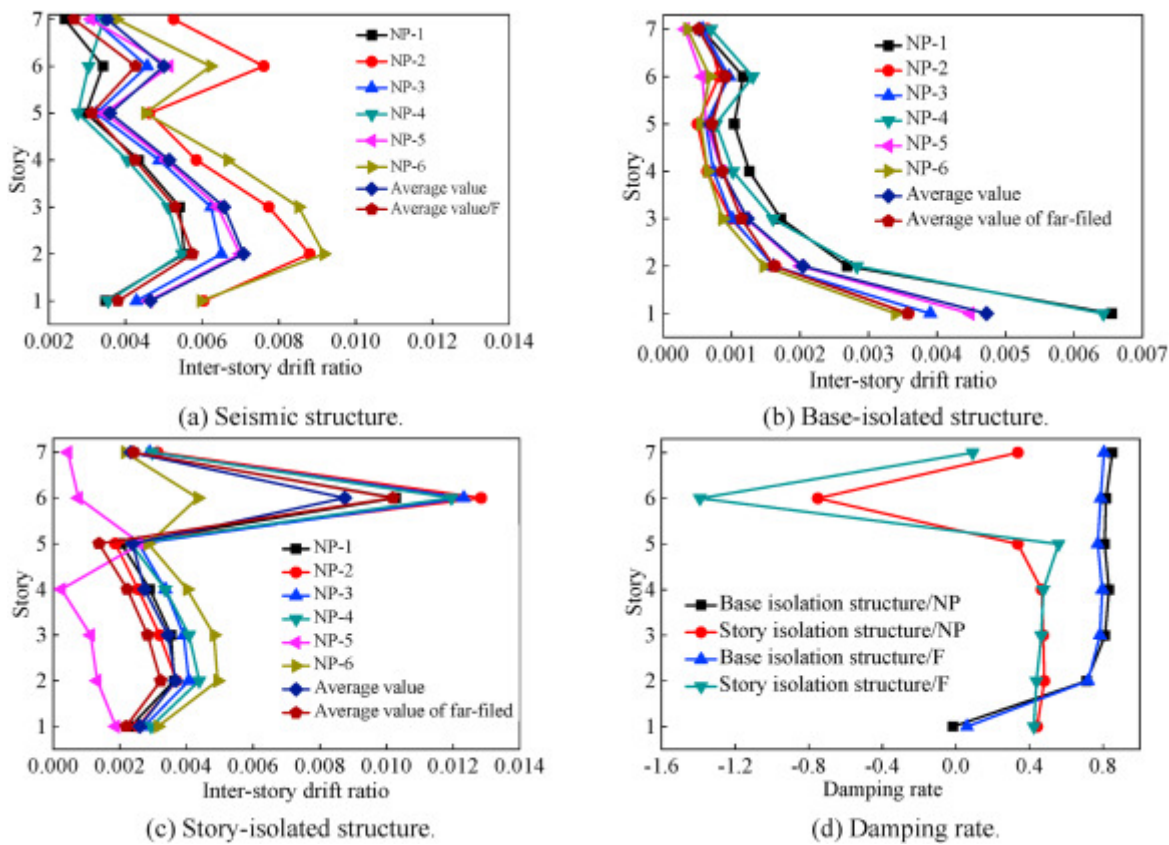
[Download : Download full-size image](#)

Fig. 6. Structural periods.

3.2. Inter-story drift ratio analysis

In order to reflect the overall deformation of the structure and the inter-story deformation, the inter-story drift ratio is set as an analysis index. The inter-story drift ratio of these three structures: seismic structures, base-isolated structures and story-isolated structures which are under the near-field earthquake are obtained through the analysis. Moreover, the average value of the inter-story drift ratio and damping rate of isolated structure under the near-field ground motions and far-field ground motions are obtained, separately, as shown in Fig. 7. The calculation method of the damping rate is shown as following:

$$\text{Damping rate} = \frac{\text{Response of seismic structures} - \text{Response of isolated structures}}{\text{Response of seismic structures}} \times 100\% \quad (8)$$



[Download : Download high-res image \(868KB\)](#)

[Download : Download full-size image](#)

Fig. 7. Inter-story drift and damping rate of structures.

As is shown in Fig. 7 that the inter-story drift ratio is gradually reduced in the direction of altitude, but since the sixth story starts to be added steel frame and the isolation bearing is arranged between the fifth story and sixth story in the story-isolated structure, lateral stiffness of the structure changes abruptly. Consequently, the inter-story drift ratio suddenly increases in the sixth story. Under the near-field ground motions, the average value of the inter-story drift ratio is more significant than that under the far-field ground motions.

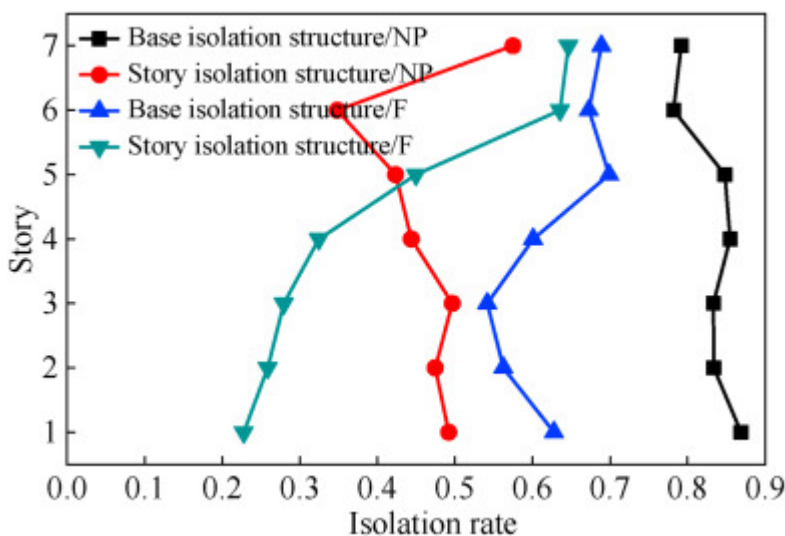
Both the base-isolated structure and the story-isolated structure shows good damping effect. Except for the isolation layer, the inter-story drift ratios are all much smaller than the seismic structure. In the isolation layer, the structural displacement is large due to the displacement of isolation bearing. Under the near-field earthquakes, the maximum damping rate of base-isolated structure is 85.02%, while the maximum damping rate of story-isolated structure is only 48.09%. It means that the damping effect of the base-isolated structures is more significant, which is because the position of isolation layer is at a higher altitude, and only the light steel frames are added above the isolation layer. Therefore, the isolation effect of the bearings is not fully utilized.

3.3. Inter-story shear force analysis

Inter-story shear force is another important indicator to measure structural seismic response, which directly reflects the performance of the isolated-structure in reducing seismic response.

By comparing the average value of the inter-story shear force of the seismic structure, the base-isolated structure, and the story-isolated structure under the near-field ground motions and far-field ground motions, it shows that there is a sudden change of inter-story shear force in the seismic structure, which because both the stiffness and quality of the light steel frame structure are much different from the lower concrete structure. Moreover, the base isolated structures and story-isolated structures can also significantly reduce the inter-story shear of the structure, this demonstrates that the abruptness of lateral stiffness problem of the adding-story structures can be solved by using isolation technique.

The shear forces of structure under the near-field pulse-like ground motions are also significantly greater than that of the far-field ground motions. From the isolation rate of structures shown in Fig. 8, whatever under near-field ground motions or far-field ground motions, the isolation effect is obvious, which means the seismic energy transfer to the upper structure above isolation layer is effectively prevented. Among them, under the near-field ground motions, the maximum isolation rate of the base-isolated structure is 86.86%, and the story-isolated structure is 57.48%; under the far-field ground motions, the maximum isolation rate of the base-isolated structure is 69.88%, and the story-isolated structure is 64.62%.



[Download : Download high-res image \(298KB\)](#)

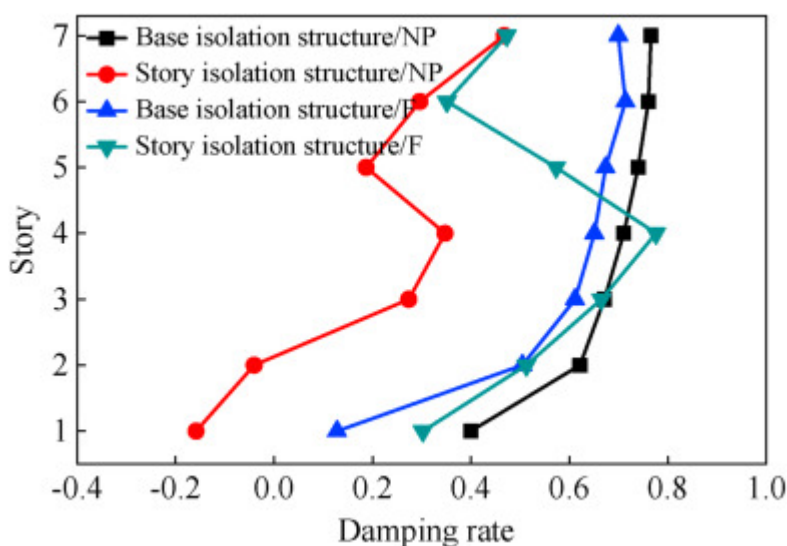
[Download : Download full-size image](#)

Fig. 8. Isolation rate of structures.

3.4. Story acceleration analysis

The average value of the acceleration amplitude of each story under the near-field ground motions and far-field ground motions is shown in Fig. 9. As shown in the figure, the accelerations of each story are gradually increased from the bottom story to the top story, and

acceleration amplitude of the top story is much larger than others. Both the seismic structures and story-isolated structures have a sudden increase in acceleration at the fifth story, and a significant inflection point appears. The acceleration of base-isolated structure changes more evenly and slowly. Moreover, the acceleration of structures under the near-field ground motions is much greater than that under the far-field ground motions. The seismic responses of the two kinds of isolated structures are significantly decreased, which indicates that the isolated structure exhibits good isolation performance. therefore, the energy transmitted to the upper structure is effectively isolated, and the acceleration of the story is minimized. However, due to the higher arrangement position of the isolation bearing, the story-isolated structure has a lower damping rate in the fifth story. Among them, under the action of near-field ground motions, the peak acceleration of seismic structure is 34.25 m/s^2 ; in contrast, the acceleration of base-isolated structure is only 8.02 m/s^2 , and the maximum damping rate is 76.57%; the acceleration of story-isolated structure is 18.04 m/s^2 , and the maximum damping rate is 46.75%. Under the far-field ground motions, the peak acceleration of seismic structure is 24.86 m/s^2 ; the structure of base isolation is 7.47 m/s^2 , and the maximum damping rate is 71.39%; the acceleration of story-isolated structure is 16.88 m/s^2 , and the maximum damping rate is 66.51%.



[Download : Download high-res image \(293KB\)](#)

[Download : Download full-size image](#)

Fig. 9. Acceleration response.

4. Discussion

From the previous analyses about the structural vibration periods, inter-story drift ratio, inter-story shear force and story accelerations, it can be concluded that the seismic influence coefficient of the structure is reduced and structural seismic response is alleviated due to the extension of structural vibration periods after arranging isolation bearings (see Table 3). The seismic responses of the isolated structures are significantly smaller than those of the seismic structure.

structures. The isolation bearings have a good damping effect on reducing the structural seismic responses, and the base-isolated structures show better damping effect. The displacements of isolated structures are shown in Table 4. It reveals that the displacements in the base-isolated structure are significantly greater than the story-isolated structure ones. So that the isolation layer of the base-isolated structure could dissipate more seismic energy than the story-isolated structures.

Table 3. Acceleration (m/s^2).

| Near-field pulse-like ground motions | | | | Far-field ground motions | | |
|--------------------------------------|-------------------|-------------------------|--------------------------|--------------------------|-------------------------|--------------------------|
| Story | Seismic structure | Base-isolated structure | Story-isolated structure | Seismic structure | Base-isolated structure | Story-isolated structure |
| 1 | 6.4653 | 3.8813 | 7.4893 | 4.1616 | 3.6288 | 3.1952 |
| 2 | 10.1333 | 3.8373 | 10.5441 | 7.5392 | 3.7360 | 4.9840 |
| 3 | 12.2053 | 4.0160 | 8.8667 | 10.1696 | 3.9504 | 6.1072 |
| 4 | 14.2747 | 4.1333 | 9.3187 | 11.8961 | 4.1521 | 6.6976 |
| 5 | 17.9267 | 4.6627 | 14.5720 | 14.2272 | 4.6432 | 9.0432 |
| 6 | 25.6107 | 6.1333 | 18.0213 | 20.1808 | 5.7744 | 14.9376 |
| 7 | 34.2481 | 8.0227 | 18.2360 | 24.8624 | 7.4688 | 16.8816 |

Table 4. Displacement in the isolated story (mm).

| | Earthquake waves | Base- isolated structure | Story-isolated structure |
|-------------------------------------|------------------|--------------------------|--------------------------|
| Near-field pulse-like ground motion | NP-1 | 134.83 | 52.37 |
| | NP-2 | 102.22 | 55.04 |
| | NP-3 | 46.26 | 68.21 |
| | NP-4 | 187.82 | 64.61 |
| | NP-5 | 148.41 | 70.00 |
| | NP-6 | 100.17 | 109.37 |
| | Average value | 119.95 | 69.93 |

| | Earthquake waves | Base- isolated structure | Story-isolated structure |
|-------------------------|-------------------------|---------------------------------|---------------------------------|
| Far-field ground motion | F-1 | 114.99 | 83.01 |
| | F-2 | 71.66 | 25.52 |
| | F-3 | 60.57 | 66.55 |
| | F-4 | 75.63 | 57.61 |
| | F-5 | 113.57 | 86.71 |
| | F-6 | 63.92 | 42.42 |
| | Average value | 83.39 | 60.30 |

In addition, the displacement of isolated structures under the near-field pulse-like ground motions are greater than that of the far-field ground motions. This probably because the long-period characteristic of isolated structures makes those structures not insensitive to the high-frequency components of non-pulse-like ground motions. The near-field ground motions contain the low-frequency component and have the characteristic of large amplitude, long cycle, and concentrated energy. When the structural natural vibration periods are close to the period pulse-like ground motions, the seismic response will be significantly amplified. Therefore, near-fault pulse-like ground motions are likely to be a severe threat to the long-period structures. The characteristic of near-field ground motions shouldn't be ignored for seismic response analysis of isolated structures.

5. Conclusions

In this paper, the isolation technique is applied to the story-adding structure with light steel frames, and the dynamic responses of the seismic structures, the base-isolated structures, and the story-isolated structures which are subjected the near-field pulse-like earthquake and far-field earthquake are analysed. It can provide a reference for the plan selection of story-adding structure through this study, especially for the structures under near-fault pulse-like ground motions. The following conclusions are drawn:

- (1) Isolation technique used in adding-story structure the periods of structure are significantly extended, and responses of both the upper structure and main structure can be reduced.
- (2) Under the action of near-field ground motion, the inter-story drift ratio decreases in the direction of structural altitude, and the average value of the inter-story drift ratio is much greater than that under the far-field ground motions.
- (3) Both base-isolated structures and story-isolated structures show good damping effect. For the reason of the higher installation location of isolation bearings, the seismic response of

the adding-story structure is somewhat amplified. The base-isolated structures show better seismic performance than the adding-story-isolated structures.

CRedit author statement

X T Ma: Conceptualization, Writing - Original Draft. **C Bao:** Writing - Original Draft. **S I Doh:** Writing - Review & Editing. **H Lu:** Software, Data Curation. **L X Zhang:** Data Curation. **Z W Ma:** Visualization. **Y T He:** Formal analysis.

Declaration of competing interest

The authors declare that they have no known competing financial interests or personal relationships that could have appeared to influence the work reported in this paper.

Acknowledgments

This project was funded by Ningxia Key Research and Development Program (Grant No. [2018BEG03009](#)), Ningxia Key Research and Development Program (Special Talents) (Grant No. [2018BEB04006](#)), Ningxia Outstanding Talent Support Program Project (Grant No. [TJGC2019001](#)), Natural Science Foundation of Ningxia (Grant No. [2020AAC03223](#)), Outstanding Young Teachers Training Foundation of Ningxia (Grant No. [NGY2020054](#)) and Qinghai Basic Research Project (Grant No. [2019-ZJ-7048](#)).

[Recommended articles](#)

[Citing articles \(0\)](#)

References

[Almufli et al., 2015](#) I. Almufli, R. Motamed, D.N. Grant, M. Willford

Incorporation of velocity pulses in design ground motions for response history analysis using a probabilistic framework

Earthq. Spectra, 31 (2015), pp. 1647-1666

[View Record in Scopus](#) [Google Scholar](#)

[Alonso-Rodríguez and Miranda, 2015](#) A. Alonso-Rodríguez, E. Miranda

Assessment of building behavior under near-fault pulse-like ground motions through simplified models

Soil Dynam. Earthq. Eng., 79 (2015), pp. 47-58

[Article](#)  [Download PDF](#) [View Record in Scopus](#) [Google Scholar](#)

[Branco and Guerreiro, 2011](#) M. Branco, L.M. Guerreiro

Seismic rehabilitation of historical masonry buildings

Eng. Struct., 33 (2011), pp. 1626-1634

[Article](#)  [Download PDF](#) [View Record in Scopus](#) [Google Scholar](#)

[Cai et al., 2016](#) Y. Cai, X. Li, S. Xue

FEEDBACK 

Application and design of 3D seismic isolation bearing in lattice shell structure

Trans. Hong Kong Inst. Eng., 23 (2016), pp. 200-213

[View Record in Scopus](#) [Google Scholar](#)

[Chen and Shen, 2014](#) Z.Y. Chen, H. Shen

Dynamic centrifuge tests on isolation mechanism of tunnels subjected to seismic shaking

Tunn. Undergr. Space Technol., 42 (2014), pp. 67-77

[Article](#)  [Download PDF](#) [View Record in Scopus](#) [Google Scholar](#)

[Cheng et al., 2017](#) X. Cheng, W. Jing, J. Chen, X. Zhang

Pounding dynamic responses of sliding base-isolated rectangular liquid-storage structure considering soil-structure interactions

Shock Vib., 2017 (2017)

[Google Scholar](#)

[Chey et al., 2013](#) M.H. Chey, J.G. Chase, J.B. Mander, A.J. Carr

Innovative seismic retrofitting strategy of added stories isolation system

Front. Struct. Civ. Eng., 7 (2013), pp. 13-23

[CrossRef](#) [View Record in Scopus](#) [Google Scholar](#)

[Chioccarelli and Iervolino, 2013](#) E. Chioccarelli, I. Iervolino

Near-source seismic hazard and design scenarios

Earthq. Eng. Struct. Dynam., 42 (2013), pp. 603-622

[CrossRef](#) [View Record in Scopus](#) [Google Scholar](#)

[Ferraioli and Mandara, 2016](#) M. Ferraioli, A. Mandara

Base isolation for seismic retrofitting of a multiple building structure: evaluation of equivalent linearization method

Math. Probl Eng., 2016 (2016)

[Google Scholar](#)

[Hasheminejad and Miri, 2008](#) S.M. Hasheminejad, A.K. Miri

Seismic isolation effect of lined circular tunnels with damping treatments

Earthq. Eng. Eng. Vib., 7 (2008), pp. 305-319

[CrossRef](#) [View Record in Scopus](#) [Google Scholar](#)

[Kanyilmaz and Castiglioni, 2017](#) A. Kanyilmaz, C.A. Castiglioni

Reducing the seismic vulnerability of existing elevated silos by means of base isolation devices

Eng. Struct., 143 (2017), pp. 477-497

[Article](#)  [Download PDF](#) [View Record in Scopus](#) [Google Scholar](#)

[Li, 2014](#) K. Li

Nonlinear analysis of seismic response on reinforced concrete frame structure with storey-adding of light-weight steel

FEEDBACK 

World Earthq. Eng., 30 (2014), pp. 82-85

[View Record in Scopus](#) [Google Scholar](#)

[Li et al., 2013](#) X. Li, S. Xue, Y. Cai

Three-dimensional seismic isolation bearing and its application in long span hangars

Earthq. Eng. Eng. Vib., 12 (2013), pp. 55-65

[CrossRef](#) [View Record in Scopus](#) [Google Scholar](#)

[Lignola et al., 2016](#) G.P. Lignola, L. Di Sarno, M. Di Ludovico, A. Prota

The protection of artistic assets through the base isolation of historical buildings: a novel uplifting technology

Mater. Struct., 49 (2016), pp. 4247-4263

[CrossRef](#) [View Record in Scopus](#) [Google Scholar](#)

[Loh et al., 2013](#) C.H. Loh, J.H. Weng, C.H. Chen, K.C. Lu

System identification of mid-story isolation building using both ambient and earthquake response data

Struct. Contr. Health Monit., 20 (2013), pp. 139-155

[CrossRef](#) [View Record in Scopus](#) [Google Scholar](#)

[Lu and Chen, 2018](#) B.J. Lu, D.Z. Chen

Application and analysis of a reinforced concrete frame topped with light-steel story

J. Hefei Univ. Technol. (Nat. Sci.), 41 (2018), pp. 390-394

[View Record in Scopus](#) [Google Scholar](#)

[Luo et al., 2016](#) H. Luo, R. Zhang, D. Weng

Mitigation of liquid sloshing in storage tanks by using a hybrid control method

Soil Dynam. Earthq. Eng., 90 (2016), pp. 183-195

[Article](#)  [Download PDF](#) [View Record in Scopus](#) [Google Scholar](#)

[Lupășteanu et al., 2019](#) V. Lupășteanu, L. Soveja, R. Lupășteanu, C. Chingălată

Installation of a base isolation system made of friction pendulum sliding isolators in a historic masonry orthodox church


Eng. Struct., 188 (2019), pp. 369-381

[Article](#)  [Download PDF](#) [View Record in Scopus](#) [Google Scholar](#)

[Ma et al., 2018](#) C. Ma, D. Lu, X. Du

Seismic performance upgrading for underground structures by introducing sliding isolation bearings

Tunn. Undergr. Space Technol., 74 (2018), pp. 1-9

[Article](#)  [Download PDF](#) [CrossRef](#) [View Record in Scopus](#) [Google Scholar](#)

[Makris, 2019](#) N. Makris

Seismic isolation: early history

Earthq. Eng. Struct. Dynam., 48 (2019), pp. 269-283

[CrossRef](#) [View Record in Scopus](#) [Google Scholar](#)

- [Mansouri and Nazari, 2017](#) S. Mansouri, A. Nazari
The effects of using different seismic bearing on the behavior and seismic response of high-rise building
Civil. Eng. J., 3 (2017), pp. 160-171
[CrossRef](#) [View Record in Scopus](#) [Google Scholar](#)
- [Petrovčič and Kilar, 2017](#) S. Petrovčič, V. Kilar
Seismic retrofitting of historic masonry structures with the use of base isolation— modeling and analysis aspects
Int. J. Architect. Herit., 11 (2017), pp. 229-246
[CrossRef](#) [View Record in Scopus](#) [Google Scholar](#)
- [Rao and Jangid, 2001](#) P.B. Rao, R.S. Jangid
Performance of sliding systems under near-fault motions
Nucl. Eng. Des., 203 (2001), pp. 259-272
[CrossRef](#) [Google Scholar](#)
- [Saha et al., 2016](#) S.K. Saha, K. Sepahv, V.A. Matsagar, A.K. Jain, S. Marburg
Fragility analysis of base-isolated liquid storage tanks under random sinusoidal base excitation using generalized polynomial chaos expansion–based simulation
J. Struct. Eng., 142 (2016), Article 04016059
[View Record in Scopus](#) [Google Scholar](#)
- [Waghmare et al., 2019](#) M.V. Waghmare, S.N. Madhekar, V.A. Matsagar
Semi-active fluid viscous dampers for seismic mitigation of RC elevated liquid storage tanks
Int. J. Struct. Stabil. Dynam., 19 (2019), p. 1950020
[CrossRef](#) [View Record in Scopus](#) [Google Scholar](#)
- [Wald et al., 1996](#) D.J. Wald, T.H. Heaton, K.W. Hudnut
The slip history of the 1994 Northridge, California, earthquake determined from strong-motion, teleseismic, GPS, and leveling data
Bull. Seismol. Soc. Am., 86 (1996), pp. S49-S70
[View Record in Scopus](#) [Google Scholar](#)
- [Wang et al., 2012](#) S.J. Wang, K.C. Chang, J.S. Hwang, J.Y. Hsiao, B.H. Lee, Y.C. Hung
Dynamic behavior of a building structure tested with base and mid-story isolation systems
Eng. Struct., 42 (2012), pp. 420-433
[Article](#)  [Download PDF](#) [View Record in Scopus](#) [Google Scholar](#)
- [Xu et al., 2020](#) Z. Xu, X. Du, C. Xu, R. Han
Numerical analyses of seismic performance of underground and aboveground structures with friction pendulum bearings
Soil Dynam. Earthq. Eng., 130 (2020), p. 105967

[Yan and Chen, 2015](#) G. Yan, F. Chen

Seismic performance of midstory isolated structures under near-field pulse-like ground motion and limiting deformation of isolation layers

Shock Vib., 2015 (2015), p. 730612

[View Record in Scopus](#) [Google Scholar](#)

[Yong-Chul et al., 2010](#) K. Yong-Chul, S. Xue, P. Zhuang, W. Zhao, C. Li

Seismic isolation analysis of FPS bearings in spatial lattice shell structures

Earthq. Eng. Eng. Vib., 9 (2010), pp. 93-102

[CrossRef](#) [View Record in Scopus](#) [Google Scholar](#)

[Zhang et al., 2011](#) R. Zhang, D. Weng, X. Ren

Seismic analysis of a LNG storage tank isolated by a multiple friction pendulum system

Earthq. Eng. Eng. Vib., 10 (2011), pp. 253-262

[CrossRef](#) [View Record in Scopus](#) [Google Scholar](#)

[Zhang et al., 2019](#) C.X. Zhang, G.B. Nie, J.W. Dai, K. Liu, X.D. Zhi, H.H. Ma

Seismic isolation research on a double-layer lattice structure using shaking table tests

International Journal of Steel Structures (2019), pp. 1-12

[Article](#)  [Download PDF](#) [CrossRef](#) [View Record in Scopus](#) [Google Scholar](#)

[Zhou et al., 2016](#) Q. Zhou, M.P. Singh, X.Y. Huang

Model reduction and optimal parameters of mid-story isolation systems

Eng. Struct., 124 (2016), pp. 36-48

[Article](#)  [Download PDF](#) [View Record in Scopus](#) [Google Scholar](#)

© 2020 Elsevier Ltd. All rights reserved.



[About ScienceDirect](#)

[Remote access](#)

[Shopping cart](#)

[Advertise](#)

[Contact and support](#)

[Terms and conditions](#)

[Privacy policy](#)

[FEEDBACK](#) 

We use cookies to help provide and enhance our service and tailor content and ads. By continuing you agree to the **use of cookies**.
Copyright © 2021 Elsevier B.V. or its licensors or contributors. ScienceDirect® is a registered trademark of Elsevier B.V.
ScienceDirect® is a registered trademark of Elsevier B.V.

